Preservation of shape discrimination in aging

Claudine Habak Centre for Vision Research, York University, Toronto, ON, Canada

Frances Wilkinson Department of Psychology and Centre for Vision Research, York University, Toronto, ON, Canada

Hugh R. Wilson Department of Biology and Centre for Vision Research, York University, Toronto, ON, Canada

The representation of objects becomes increasingly complex at higher levels of the human visual cortex. Shapes of intermediate complexity serve as a step in the representation of such intricate constructs. Healthy aging has adverse effects on cortical function, and we sought to determine the effects of age on the efficacy and speed of neuronal mechanisms underlying shape processing. Using deformed circular shapes, we probe object representation by varying the characteristics that define the shape and by assessing lateral interactions among shapes. Results indicate that performance declines with age for shapes defined by texture but not by luminance. However, there is no age-related slowing for the processing of shape, and probes of lateral interactions reveal spared function for complex shape combinations. Findings suggest that the effect of age on shapes defined by texture arises from lower stages of visual processing, and that the representation of shape combinations is spared because of its robust nature.

Keywords: aging, shape perception, first order, second order, lateral masking, temporal vision, face perception

Citation: Habak, C., Wilkinson, F., & Wilson, H. R. (2009). Preservation of shape discrimination in aging. *Journal of Vision, 9*(12):18, 1–8, http://journalofvision.org/9/12/18/, doi:10.1167/9.12.18.

Introduction

A gradual decline in visual abilities is common even in healthy aging. These changes may be explained, in part, by optical characteristics of the aging eye (Weale, 1963) but are attributed mainly to neural changes in the aging brain (Ball & Sekuler, 1986; Habak & Faubert, 2000; Sekuler & Sekuler, 2000; Spear, 1993). For example, neuronal activity in aging macaque V1 displays an increase in spontaneous firing, a decrease in signal-to-noise ratio, and a decrease of selectivity for both orientation and motion direction (Leventhal, Wang, Pu, Zhou, & Ma, 2003; Schmolesky, Wang, Pu, & Leventhal, 2000), all of which are exacerbated in V2 (Yu, Wang, Li, Zhou, & Leventhal, 2006). Basic sensitivities mediated by early stages of visual processing, such as contrast and spatial frequency, deteriorate with age (Owsley, Sekuler, & Siemsen, 1983). Aging also affects complex representations such as face perception (Habak, Wilkinson, & Wilson, 2008; Lott, Haegerstrom-Portnoy, Schneck, & Brabyn, 2005; Owsley, Sekuler, & Boldt, 1981), which rely upon higher stages of the object-processing stream. Surprisingly, thresholds for detecting deformation of circular shapes, which are hyperacuities in young adults (Wilkinson, Wilson, & Habak, 1998), appear to be preserved into advanced age, at least for low radial frequencies (Wang, 2001; Wang, Wilson, Locke, & Edwards, 2002). The global pooling of contour information underlying this task is thought to occur at intermediate levels of the ventral pathway (Gallant, Shoup, & Mazer, 2000; Wilkinson et al., 2000), yet the optical and neural degradation of the input associated with aging do not appear to impair this ability. However, Wang et al.'s studies used only luminance-defined radial frequency (RF) contours, and stimulus exposure time was relatively long (500 ms minimum).

When contours are defined by contrast or texture change (second order or non-Fourier), sensitivity to local orientation (Lin & Wilson, 1996), to curvature (Wilson & Richards, 1992), and to global shape (Bell & Badcock, 2008; Hess, Achtman, & Wang, 2001) are reduced relative to luminance-defined (first order or Fourier) contours in young adults. Thresholds for detecting changes in these properties are generally 2–8 times higher for second-order stimuli. This is likely due to larger receptive fields pooling signals from local orientation-tuned neurons and secondly to noise associated with an extra stage of processing. Furthermore, the time required to integrate second-order information to achieve optimal performance is longer than for luminance contours (Lin & Wilson, 1996). Finally, contour information is integrated globally for shapes defined by first-order (Bell & Badcock, 2008; Loffler, Wilson, & Wilkinson, 2003) and by second-order characteristics (Bell & Badcock, 2008).

Reduced processing speed has been suggested as a common factor underlying many of the cognitive changes

doi: 10.1167/9.12.18 Received August 7, 2009; published November 23, 2009 ISSN 1534-7362

accompanying aging (Cerella, 1985; Salthouse, 1996). Physiological evidence is consistent with this suggestion. Changes in myelination throughout monkey cortex, including visual cortex, could lead to slower or asynchronous signal transmission and have been linked to behavioral change (Peters, 2002; Peters, Verderosa, & Sethares, 2008). Secondly, the accumulation of information in neuronal populations might occur over longer periods of time because aging neurons exhibit a lower signal-to-noise ratio (Yu et al., 2006). Physiological recordings indicate that intracortical processing and transfer rates slow with advanced age in V1 efferent layers and to a larger extent in V2 (Wang, Zhou, Ma, & Leventhal, 2005). Therefore, differences in performance between older and younger observers might be revealed or exacerbated as stimulus durations are shortened. In the first part of the present study we revisit the issue of radial frequency sensitivity in healthy aging, measuring thresholds for detecting deviations from circularity for both luminance and texture-defined shapes at a range of exposure times.

Reduced signal-to-noise ratio in visual cortex could arise through the reduction in GABA-mediated intracortical inhibition, which has been reported to occur in aging (Leventhal et al., 2003). It has been argued (Betts, Taylor, Sekuler, & Bennett, 2005) that in certain circumstances weakened inhibition may actually lead to superior performance in elderly individuals. Specifically, they reported that the surround suppression that leads to poorer direction discrimination for large, high contrast moving targets than for small targets (Tadin, Lappin, Gilroy, & Blake, 2003) is less marked in elderly individuals; thus their motion sensitivity is actually better than that of younger subjects under this stimulus condition. In previous work in our laboratory, we have shown that detection thresholds for radial frequency patterns are very sensitive to lateral masking by high amplitude RF patterns matched in radial frequency and phase to the target (Habak, Wilkinson, Zakher, & Wilson, 2004). In the second part of the present study, we ask whether this shape-specific lateral masking is reduced in healthy older subjects in the same way that motion surround inhibition is (Betts et al., 2005).

Methods

Participants

Eighteen younger observers (mean age 23.1 years, *SD* ± 2.9, range 20–30) and eighteen community dwelling older observers (mean age 65.2 years, *SD* ± 4.3, range 60–76) participated in this study. Older observers were screened for general health and for medications that could affect visual or brain function. They also underwent complete eye exams by an optometrist and only those with healthy eyes participated in these experiments. Corrected visual acuity was 20/20 or better in all participants with the exception of one observer in each group, who had visual acuity of 20/25. Older observers were corrected for the viewing distance of 131 cm. Participation was voluntary, and the study was approved by York University's Human Participants Review Committee.

Apparatus and stimuli

Stimuli were presented on an Apple iMac G3 using custom Matlab software incorporating routines from the Psychophysics and Video Toolbox (Brainard, 1997; Pelli, 1997). Monitor resolution was set to 1024 × 768 with a refresh rate of 75 Hz. The monitor was calibrated so that contrasts were linearized using 151 equally spaced gray levels. The monitor was viewed binocularly from a distance of 131 cm, so one pixel subtended 41.5 arcsec. The mean luminance was 65 cd/m^2.

Stimuli consisted of radial frequency (RF) patterns (Figure 1), which are closed contours defined as a sinusoidal modulation of a circle's radius according to the following equation (Wilkinson et al., 1998):

$$r(\theta) = r_{\text{mean}}(1 + A\sin(\omega\theta + \phi)), \quad (1)$$

where r and θ are the polar coordinates of the contour, and r_{mean} is the average radius (radius of the base circle). The remaining three parameters control various aspects of the shape's geometry, where ω is the radial frequency, which represents the integer number of sinusoidal modulation cycles (peaks and troughs about the circle), ϕ is the phase, which represents the overall orientation of the shape, and A is the amplitude and represents the size of these deformations as a proportional change of the radius. The radial frequency of all contours was 5 cycles/circumference, and the mean radius was 1° of visual angle.

For the first-order patterns, the cross-sectional luminance profile of the contour consisted of a fourth derivative of a Gaussian (D4; see Wilkinson et al., 1998 for details) with a peak spatial frequency of 4 cpd (bandwidth = 1.24 cycles) and luminance contrast of 90%. To create the second-order contours, a radially modulated Gaussian window was multiplied with a radial carrier grating (Habak et al., 2004) of 4 cpd spatial frequency and 90% luminance contrast (Figure 1b). In addition, noise masks consisting of binary noise filtered with the same characteristics and peak spatial frequency (4 cpd) as the contours were used; root mean square contrast was adjusted to match that of the contours. Noise mask presentation is detailed below in the Procedure section.

For conditions evaluating lateral interactions among shapes, target and mask contours each had a radial

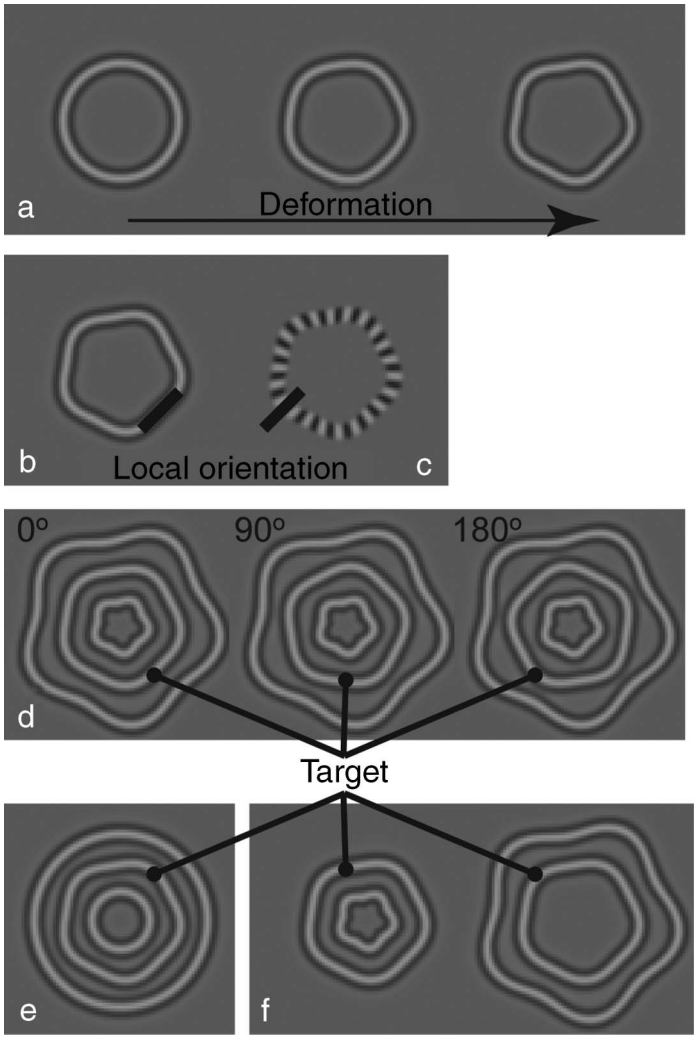

Figure 1. (a) D4 contours describing a circle and RF5 patterns of increasing amplitude. (b) First-order and (c) second-order RF5 patterns of equal amplitude; local orientation at one point along the contour is illustrated by black bars. Local orientation of the carrier texture (c) is orthogonal to the RF contour. (d) Pair of RF masks, one surrounding and the other lying inside the target, matched to the target in radial frequency and either in phase with the target (0°) or rotated 90° or 180° relative to the target. (e) RF5 target with circular masks. (f) RF5 target with a single inner or outer mask.

frequency of 5 cycles. Target mean radius was 1°, RF masks smaller than the target (inner masks) had a mean radius of 0.5° and those larger than the target (outer masks) a mean radius of 1.5°. Mask deformation amplitude was set to 15× deformation threshold for each observer (Figures 1d and 1f). In the case of the double RF mask (inner and outer, Figure 1d), the masks were presented in 3 phases relative to the target RF5 pattern: in phase (0°), 90° and 180° out of phase. Circle mask (RF0; Figure 1e) position was equated to the minimum distance between target and RF masks: the distance between mask concavities and the target for the outer masks, and the distance between mask convexities and the target for the inner masks. The spatial location of the patterns was jittered slightly (15 pixels), so that observers could not attend to a specific portion of the stimulus and had to make a judgment on its global shape.

Procedure

Target deformation detection thresholds, or amplitude of the minimum detectable distortion, were measured. The method of constant stimuli was used in a two-interval temporal forced choice paradigm, with an inter-stimulus blank period (mean gray) of 300 ms. One interval contained a true circle and the other, the RF deformed circle. In all conditions, the observer's task was to indicate which interval contained the modulated RF pattern. Young observers indicated their choice by pressing "1" or "2" on the keyboard; to avoid key-press errors, the experimenter entered the older observers' verbal responses. Baseline thresholds for first- and second-order contours were collected with stimulus durations of 500 ms. For the conditions assessing processing speed, each contour was shown for one of three durations (40, 120, and 360 ms) and was followed immediately by a 360-ms exposure of the corresponding random noise mask to interrupt further processing of the contour. Within a block of trials (1 run), four to six levels of circular deformation were each shown 15 times, for a total of 60–90 trials per condition. In the lateral masking portion of the study, four masking conditions were tested with order randomized across older subjects. Each young subject was given the same test sequence as one of the older subjects (yoked control). The four conditions were pairs of RF masks (Figure 1d), pairs of circles (Figure 1e), and single inner and outer RF masks (Figure 1f). In the case of the paired RF masks, the phase of the target RF relative to the mask was randomized.

Baseline thresholds for first-order RF patterns were measured first in all participants. This was followed by the lateral masking conditions, with order randomized across individuals. The block containing the double RF mask contained three times as many trials as the other conditions; within this condition, 0°, 90°, and 180° mask rotations were randomly intermixed. The inner and outer masks were always matched in phase (Figure 1d). In a second test session, deformation thresholds for the second-order RF5 stimulus were measured with 500-ms unmasked stimulus exposures. This was followed by threshold measurement in the six limited exposure conditions (40-, 120-, and 360-ms exposures for first- and second-order RF5 patterns). Again testing order was randomized across older observers; testing order for each young observer was yoked to that of an older subject. Typically testing was completed in 2 sessions each lasting 1.5 h; however, in some cases, testing was extended over 3 or more sessions if participants found the testing tiring.

Observers were given at least one practice run of 25 trials before beginning each new task.

Data analysis

Data from each block were fit with a Quick (Quick, 1974) or Weibull (Weibull, 1951) function using maximum likelihood estimation, and thresholds were estimated at 75% correct responses. Split plot analyses of variance (ANOVA) were carried out on log-transformed thresholds. In cases in which the sphericity assumption was not met, the Geisser–Greenhouse adjustment to the degrees of freedom was employed. Post-hoc comparisons were conducted using Tukey's method with the α level set to <0.05.

Results

Contour type and stimulus duration

In Figure 2, red and blue circles represent thresholds (expressed in seconds of arc) for luminance-defined RF contours for young and older observers, respectively. Thresholds for the 500-ms unmasked stimuli were approximately 10 s of arc for both groups, confirming previous reports of hyperacuity performance in both young and elderly observers for similar patterns (Wang, 2001; Wilkinson et al., 1998). Split plot ANOVA (two age groups (between groups factor) × four exposure times (repeated measure)) revealed that there was no main effect of age group (F = 0.34; p = 0.56) and no interaction between age and target duration (F = 0.47; p = 0.71). The main effect of target duration was highly significant ($F_{[1,17]}$ = 111.2, p < 0.0001) with performance declining at shorter exposures. Post-hoc tests revealed that performance showed a significant improvement between exposure durations of 40 and 120 ms and between 120 and 500 ms but not between 360 and 500 ms. To achieve an estimate of asymptotic performance on this task, the geometric means for each group were fit with an exponential function that decays to an asymptotic level. The asymptotic thresholds for young and older groups were 10.5 and 10.6 s of arc, respectively; the associated time constants were 42.1 and 43.2 ms.

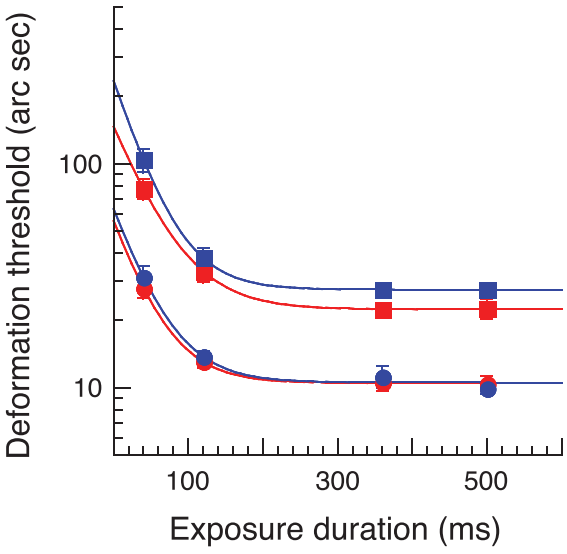

Figure 2. Deformation detection thresholds for young (red) and older (blue) participants for RF5 shapes defined by first-order (circles) or second-order (squares) contours. Amplitude thresholds for the minimum detectable distortion are expressed in seconds of arc. Error bars: 1 standard error.

Thresholds for second-order stimuli (Figure 2, square symbols) were approximately 3 times worse than first-order thresholds for both age groups and all exposure durations. Split plot ANOVA for the second-order stimuli revealed significant main effects of both age (F = 10.99; p < 0.002) and exposure time (F = 103.2; p < 0.0001) but no interaction between age and exposure time (F = 0.008; p = 0.81). Performance of older subjects was worse than that of younger individuals at all stimulus durations. As was the case for first-order stimuli, post-hoc comparisons revealed that performance with second-order stimuli showed a significant improvement between exposure durations of 40 and 120 ms and between 120 and 360 ms but not between 360 and 500 ms. When decaying exponential functions were fit to the means, asymptotic thresholds for the second-order stimuli were estimated at 22.4 s and 27.5 s of arc for young and older subjects, respectively (time constants: 49.2 and 40.4 ms). Using the pooled variance from all second-order test conditions, we calculated the 95% confidence limits around the estimated mean for the young group (22.4 s) and found that the estimate for the older subjects (27.5 s) lies outside the upper bound of this confidence interval.

Lateral masking among shapes

In Figure 3, open and filled circles represent thresholds for young and older subjects, respectively, tested without masks (No Mask) and with a variety of masking contours. The No Mask results are the data from the 500-ms condition from the luminance contour data set described above and in Figure 2; the shaded region represents the 95% confidence limits for this No Mask baseline condition. Thresholds in the No Mask condition were compared to thresholds under the six lateral masking conditions in a split plot ANOVA with age as the between-group factor and mask condition the within-subject measure. The main effect of mask condition was significant ($F_{[6,204]}$ = 63.95, p < 0.0001); however, the effect of age was not statistically significant (F = 0.2518;

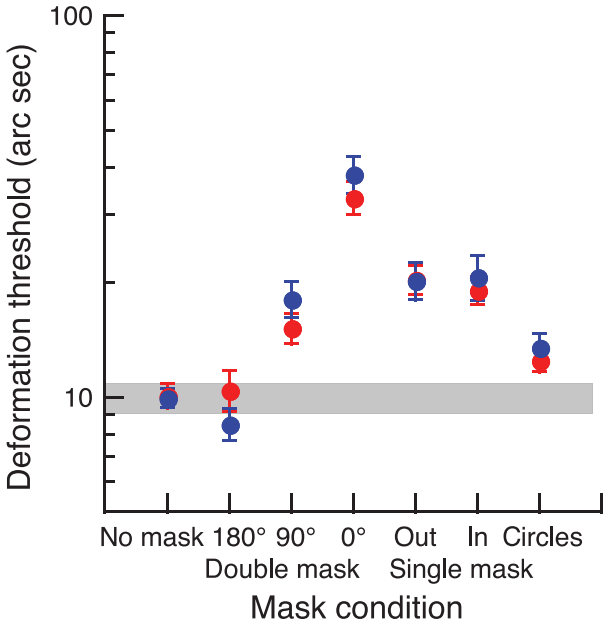

Figure 3. Deformation thresholds for young (red) and older (blue) participants with no spatial masks and under six mask conditions. The paired RF masks were either in phase with the test RF contour (0°) or 90° or 180° out of phase. The single RF mask lay either outside (Out) or inside (In) the test contour (see Figures 1d and 1f). The shaded area represents the 95% confidence interval for the baseline condition. Error bars: 1 standard error.

$p = 0.61$), nor was the interaction between age and mask condition ($F = 1.19$; $p = 0.31$). Post-hoc comparisons using Tukey's method were employed to examine the relative strengths of various mask configurations.

As can be seen in Figure 3, the strongest masking was exerted by the pair of RF5 masks when they were in phase with the test RF. The strength of this masking declines when the masks are 90° out of phase with the test RF and masking disappears completely when the masks are rotated to 180° out of phase (90° mask differs significantly from both in-phase and 180° rotated masks; 180° does not differ from No Mask). When a single in-phase RF mask was used, masking was reduced to about half the strength of the double mask condition. Both inner and outer single masks exerted significant masking relative to the No Mask condition, but there was no difference in masking strength between inner and outer masks. Finally, a double mask composed of circles exerted a small masking effect relative to the No Mask condition, but this did not reach statistical significance.

Discussion

A probe of the mechanisms underlying shape perception reveals that aging can lead to degraded perception of shapes defined by second-order characteristics (texture). In contrast, the thresholds for the perception of the same shapes defined by first-order characteristics (luminance), the speed of processing underlying shape perception, and the strength of lateral interactions among shapes do not change with age, at least over the range tested here.

Defining properties of shape and timing

The finding of normal RF detection thresholds in the older group for luminance defined patterns at long (500 ms) exposures supports an earlier report by Wang (2001) and extends the finding to brief exposures (down to 40 ms). Previous work from our laboratory and others has shown that optimal performance on this task, which fall in the hyperacuity range, involves global pooling of orientation/curvature information around the entire pattern (Bell & Badcock, 2008; Hess, Wang, & Dakin, 1999; Loffler et al., 2003; Wilkinson et al., 1998); intermediate levels of the ventral visual pathway have been implicated in this pooling process (Gallant, Connor, Rakshit, Lewis, & Van Essen, 1996; Gallant et al., 2000; Wilkinson et al., 2000). The present findings indicate that these central pooling processes are not degraded in aging, at least not over the age range studied here, and in the absence of peripheral pathology.

On the other hand, the small but significant deficit in detection of RF shapes defined by second-order contours indicates that aging does incur some cost. This deficit in texture processing is in line with the deficit reported previously in second-order motion perception by Habak and Faubert (2000) in an elderly population. While texture-based deficits can sometimes be attributed to acuity or contrast sensitivity limitations, that is unlikely in the present case. The radial grating pattern used as the carrier of the second-order RF pattern was matched in spatial frequency to the peak spatial frequency (4 cpd) of the contour defining the first-order patterns, and both were of high contrast. It is important to emphasize that deficits of equivalent severity occurred at all exposure intervals, as illustrated in Figure 2. There are suggestions in the literature that slowed processing may be one hallmark of aging (Salthouse, 1996); however, in the present case, performance of the young and old groups does not converge at long exposure as would be expected in such a situation; rather the deficit persists even when asymptotic performance has been achieved.

It must be emphasized that our procedure removed any confound of slowed response times as our measure did not involve reaction time. Moreover, by having an experimenter enter the verbal responses of the older subjects, keyboard errors due to motor or tactile problems were avoided. Thus the deficiency most likely occurs in the visual pathway at the stage at which local orientation

signals are pooled by neurons acting as second stage filters encoding the orientation of the texture-defined contour. A probable neural site for this abnormality would be in cortical area V2. Although orientation tuning has been shown to be broadened in both V1 and V2 in very old primates (Schmolesky et al., 2000; Yu et al., 2006), these effects are significantly greater in V2 as are other neural changes such as increased spontaneous activity levels, increased response latency, and elevated maximum firing rate (Wang et al., 2005). Either less selective responses to the orientation of texture boundaries or other forms of increased neural noise could contribute to the elevated shape detection thresholds in the older subjects by providing less accurate signals to the stage at which global pooling occurs. Second-order contours can only be integrated optimally over slightly larger areas than first-order contours (Bell & Badcock, 2008) and could be especially sensitive to age-related decreases in orientation selectivity. At the level at which shape discriminations of the type examined here are performed, it appears that shapes derived from first-order and from second-order stimuli share a common representation: masking of the type discussed below occurs as strongly between first- and second-order stimuli as among first-order contours (Bell & Badcock, 2008; Habak et al., 2004). Thus it appears that it is the second-order input to this mechanism that is affected rather than the shape processing itself.

Lateral masking and inhibition

The results for masking interactions in the young participants largely replicate our earlier findings (Habak et al., 2004), showing strong masking by high amplitude RF patterns matched in radial frequency and phase to the target. As in our previous work, the strength of masking was found to decline as the phase relationship between masks and target is altered, disappearing completely when they are 180 deg out of phase. Circular masks did not exert a significant masking effect, again replicating our earlier findings. The absence of strong masking by circles is important because at their detection threshold, the RF target patterns are much more similar to the circular masks in terms of the local orientations and local curvatures along the contours than they are to their matching in-phase RF masks (see Figure 1), which did exert strong masking. Moreover, the stimuli were designed such that the circular masks were spatially as close to the targets at every point as the RF masks were at their closest points (concavities for the outer masks; convexities for the inner masks).

Age did not produce a significant change in the strength of this shape-specific masking. As described earlier, there is evidence that in the motion pathway surround suppression effects are weakened by aging (Betts et al., 2005). It has been suggested that this may be due to the demonstrated reduction in GABA-mediated intracortical inhibition in older brains (Hua, Kao, Sun, Li, & Zhou, 2008; Leventhal et al., 2003). Were analogous lateral interactions relevant in the present case, we might have expected superior performance in our older participants in the masking conditions. As is evident in Figure 3, this was not the case. We detected no statistically significant differences in masking, and any trend in the data is toward stronger, not weaker, masking in the older participants. This provides further support for the conclusion we have reached in our earlier work that the interactions involved in this "shape masking" do not involve local orientation-based or local curvature-based inhibitory interactions of the sort that might arise in V1 or V2. Instead, we would argue that these interactions occur higher in the ventral visual pathway, most likely in area V4, or possibly in some portion of inferotemporal cortex or, in humans, LO. Both recent empirical data (Dumoulin & Hess, 2007; Gallant, Braun, & Van Essen, 1993; Gallant et al., 1996; Pasupathy & Connor, 1999) and recent modeling (Cadieu et al., 2007; David, Hayden, & Gallant, 2006) studies of V4 emphasize the importance of curvature coding at this level along with some degree of translational invariance. Gallant's electrophysiological data emphasized the effectiveness of sets of concentric circles as stimuli for a substantial subgroup of V4 neurons (Gallant et al., 1993, 1996), and our own earlier work showed that concentric sets of RF patterns are also strong stimuli for V4 in humans (Wilkinson et al., 2000). Our earlier psychophysical data (Habak et al., 2004), and the single unit results of Pasupathy and Connor (2002, 1999), suggest that convex curves are encoded relative to the center of objects (in our case circles). These findings together suggest that distortion amplitude, meaning change in curvature relative to that of the related circle, might be what is coded by these neurons. If greater distortion amplitude produced stronger responses and if these responses were pooled over any contours lying within a sector of a circle, then relatively weak signals generated by circle arcs would have little effect on detection of small distortions in one of the arcs, whereas arcs with large distortions would significantly elevate the threshold for detecting a small distortion, much as contrast pedestals in V1 produce elevations in contrast thresholds. We have proposed a similar form of coding for representing the identity and distinctiveness of faces in the fusiform face area (Loffler, Yourganov, Wilkinson, & Wilson, 2005). To date we know of no electrophysiological or imaging data that directly address this question with respect to the coding of curved segments of contours, although superficially Pasupathy's studies suggest that in V4, neurons are tuned to specific amounts of convex or concave curvature. In the scenario we propose, the masking arises from the pooling of curvature-tuned inputs, not through lateral inhibition. While such processes might also be subject to degradation during the aging process, for example with increased neuronal firing rates and

reduced signal-to-noise ratios, the present data suggest that such effects are negligible over the age range we have investigated.

Conclusions

The findings reported here were obtained from a population of healthy older individuals who had no known peripheral eye disease and normal visual acuity. This allows us to conclude that, for the measures in question, intermediate level functions do not lead lower level ones in showing age-related degradation, although for other measures such a pattern has been reported to be the case. Finally, it should be emphasized that the seniors in our study are the "younger elderly"; that is, they ranged in age from 60 to 75. Visual functions other than acuity have been found to show their most precipitous changes in individuals in their eighties and beyond (Haegerstrom-Portnoy, 2005), so it will be of great interest to apply the same measures to an older sample.

Acknowledgments

This work was supported by NIH Grant (EY002158) and NSERC Grant (OP227224) to HRW, NSERC Grant (OP0007551) to FW, and by a CIHR Postdoctoral Fellowship to CH.

Commercial relationships: none.
Corresponding author: Claudine Habak.
Email: Claudine.Habak@umontreal.ca.
Address: Centre de Recherche, Institut Universitaire de Gériatrie de Montréal, 4545 Queen-Mary, Montréal, QC H3W 1W5, Canada.

References

Ball, K., & Sekuler, R. (1986). Improving visual perception in older observers. *Journal of Gerontology, 41,* 176–182. [PubMed]

Bell, J., & Badcock, D. R. (2008). Luminance and contrast cues are integrated in global shape detection with contours. *Vision Research, 48,* 2336–2344. [PubMed]

Betts, L., Taylor, C., Sekuler, A., & Bennett, P. (2005). Aging reduces center–surround antagonism in visual motion processing. *Neuron, 45,* 361–366. [PubMed]

Brainard, D. H. (1997). The psychophysics toolbox. *Spatial Vision, 10,* 433–436. [PubMed]

Cadieu, C., Kouh, M., Pasupathy, A., Connor, C., Riesenhuber, M., & Poggio, T. (2007). A model of V4 shape selectivity and invariance. *Journal of Neurophysiology, 98,* 1733–1750. [PubMed]

Cerella, J. (1985). Information processing rates in the elderly. *Psychological Bulletin, 98,* 67–83. [PubMed]

David, S. V., Hayden, B. Y., & Gallant, J. L. (2006). Spectral receptive field properties explain shape selectivity in area V4. *Journal of Neurophysiology, 96,* 3492–3505. [PubMed]

Dumoulin, S. O., & Hess, R. F. (2007). Cortical specialization for concentric shape processing. *Vision Research, 47,* 1608–1613. [PubMed]

Gallant, J. L., Braun, J., & Van Essen, D. C. (1993). Selectivity for polar, hyperbolic, and Cartesian gratings in macaque visual cortex. *Science, 259,* 100–103. [PubMed]

Gallant, J. L., Connor, C. E., Rakshit, S., Lewis, J. W., & Van Essen, D. C. (1996). Neural responses to polar, hyperbolic, and Cartesian gratings in area V4 of the macaque monkey. *Journal of Neurophysiology, 76,* 2718–2739. [PubMed]

Gallant, J. L., Shoup, R. E., & Mazer, J. A. (2000). A human extrastriate area functionally homologous to macaque V4. *Neuron, 27,* 227–235. [PubMed]

Habak, C., & Faubert, J. (2000). Larger effect of aging on the perception of higher-order stimuli. *Vision Research, 40,* 943–950. [PubMed]

Habak, C., Wilkinson, F., & Wilson, H. (2008). Aging disrupts the neural transformations that link facial identity across views. *Vision Research, 48,* 9–15. [PubMed]

Habak, C., Wilkinson, F., Zakher, B., & Wilson, H. (2004). Curvature population coding for complex shapes in human vision. *Vision Research, 44,* 2815–2823. [PubMed]

Haegerstrom-Portnoy, G. (2005). The Glenn A. Fry award lecture 2003: Vision in elders—summary of findings of the SKI study. *Optometry and Vision Science, 82,* 87–93. [PubMed]

Hess, R. F., Achtman, R. L., & Wang, Y. Z. (2001). Detection of contrast-defined shape. *Journal of the Optical Society of America A, Optics, Image Science, and Vision, 18,* 2220–2227. [PubMed]

Hess, R. F., Wang, Y. Z., & Dakin, S. C. (1999). Are judgements of circularity local or global? *Vision Research, 39,* 4354–4360. [PubMed]

Hua, T., Kao, C., Sun, Q., Li, X., & Zhou, Y. (2008). Decreased proportion of GABA neurons accompanies age-related degradation of neuronal function in cat striate cortex. *Brain Research Bulletin, 75,* 119–125. [PubMed]

Leventhal, A. G., Wang, Y. C., Pu, M. L., Zhou, Y. F., & Ma, Y. Y. (2003). GABA and its agonists improved

visual cortical function in senescent monkeys. *Science, 300,* 812–815. [PubMed]

Lin, L. M., & Wilson, H. R. (1996). Fourier and non-Fourier pattern discrimination compared. *Vision Research, 36,* 1907–1918. [PubMed]

Loffler, G., Wilson, H. R., & Wilkinson, F. (2003). Local and global contributions to shape discrimination. *Vision Research, 43,* 519–530. [PubMed]

Loffler, G., Yourganov, G., Wilkinson, F., & Wilson, H. (2005). fMRI evidence for the neural representation of faces. *Nature Neuroscience, 8,* 1386–1391. [PubMed]

Lott, L. A., Haegerstrom-Portnoy, G., Schneck, M. E., & Brabyn, J. A. (2005). Face recognition in the elderly. *Optometry and Vision Science, 82,* 874–881. [PubMed]

Owsley, C., Sekuler, R., & Boldt, C. (1981). Aging and low-contrast vision: Face perception. *Investigative Ophthalmology & Visual Science, 21,* 362–365. [PubMed]

Owsley, C., Sekuler, R., & Siemsen, D. (1983). Contrast sensitivity throughout adulthood. *Vision Research, 23,* 689–699. [PubMed]

Pasupathy, A., & Connor, C. (2002). Population coding of shape in area V4. *Nature Neuroscience, 5,* 1332–1338. [PubMed]

Pasupathy, A., & Connor, C. E. (1999). Responses to contour features in macaque area V4. *Journal of Neurophysiology, 82,* 2490–2502. [PubMed]

Pelli, D. G. (1997). The VideoToolbox software for visual psychophysics: Transforming numbers into movies. *Spatial Vision, 10,* 437–442. [PubMed]

Peters, A. (2002). The effects of normal aging on myelin and nerve fibers: A review. *Journal of Neurocytology, 31,* 581–593. [PubMed]

Peters, A., Verderosa, A., & Sethares, C. (2008). The neuroglial population in the primary visual cortex of the aging rhesus monkey. *Glia, 56,* 1151–1161. [PubMed]

Quick, R. F. (1974). A vector-magnitude model of contrast detection. *Kybernetik, 16,* 65–67. [PubMed]

Salthouse, T. A. (1996). The processing-speed theory of adult age differences in cognition. *Psychological Review, 103,* 403–428. [PubMed]

Schmolesky, M. T., Wang, Y., Pu, M., & Leventhal, A. G. (2000). Degradation of stimulus selectivity of visual cortical cells in senescent rhesus monkeys. *Nature Neuroscience, 3,* 384–390. [PubMed]

Sekuler, R., & Sekuler, A. B. (2000). Visual perception and cognition. In J. Evans, T. Wiliams, B. Beattie, J.-P. Michel, & G. Wilcock (Eds.), *Oxford textbook of geriatric medicine* (2nd ed., pp. 874–880). Oxford, UK: Oxford University Press.

Spear, P. D. (1993). Neural bases of visual deficits during aging. *Vision Research, 33,* 2589–2609. [PubMed]

Tadin, D., Lappin, J. S., Gilroy, L. A., & Blake, R. (2003). Perceptual consequences of center–surround antagonism in visual motion processing. *Nature, 424,* 312–315. [PubMed]

Wang, Y., Zhou, Y., Ma, Y., & Leventhal, A. G. (2005). Degradation of signal timing in cortical areas V1 and V2 of senescent monkeys. *Cerebral Cortex, 15,* 403–408. [PubMed]

Wang, Y.-Z. (2001). Effects of aging on shape discrimination. *Optometry and Vision Science, 78,* 447–454. [PubMed]

Wang, Y.-Z., Wilson, E., Locke, K. G., & Edwards, A. O. (2002). Shape discrimination in age-related macular degeneration. *Investigative Ophthalmology & Visual Science, 43,* 2055–2062. [PubMed] [Article]

Weale, R. (1963). *The aging eye*. London: H. K. Lewis.

Weibull, W. (1951). A statistical distribution function of wide applicability. *Journal of Applied Mechanics, 18,* 292–297.

Wilkinson, F., James, T. W., Wilson, H. R., Gati, J. S., Menon, R. S., & Goodale, M. A. (2000). An fMRI study of the selective activation of human extrastriate form vision areas by radial and concentric gratings. *Current Biology, 10,* 454–458. [PubMed]

Wilkinson, F., Wilson, H. R., & Habak, C. (1998). Detection and recognition of radial frequency patterns. *Vision Research, 38,* 3555–3568. [PubMed]

Wilson, H. R., & Richards, W. A. (1992). Curvature and separation discrimination at texture boundaries. *Journal of the Optical Society of America A, Optics and Image Science, 9,* 1653–1662. [PubMed]

Yu, S., Wang, Y., Li, X., Zhou, Y., & Leventhal, A. (2006). Functional degradation of extrastriate visual cortex in senescent rhesus monkeys. *Neuroscience, 140,* 1023–1029. [PubMed]